JOURNAL OF GEOPHYSICAL RESEARCH, VOL. 106, NO. D16, PAGES 18,371–18,379, AUGUST 27, 2001

# April 1998 Asian dust event: A southern California perspective

David M. Tratt
Jet Propulsion Laboratory, California Institute of Technology, Pasadena, California

Robert J. Frouin
Scripps Institution of Oceanography, University of California, San Diego, La Jolla, California

Douglas L. Westphal
Marine Meteorology Division, Naval Research Laboratory, Monterey, California

**Abstract.** In late April 1998 an extreme Asian dust episode reached the U.S. western seaboard. This event was observed by several in situ and remote sensing atmospheric measurement stations. Dramatic reductions in boundary layer visibility were recorded and the resultant peak backscatter coefficients exceeded prevailing upper tropospheric background conditions by at least 2 orders of magnitude. An analysis of this event is given using lidar vertical backscatter profilometry, concurrent Sun photometer opacity data, and transport modeling. At San Nicolas Island the measured and modeled aerosol optical thickness at 500 nm increased dramatically from 0.15 on April 25 to 0.52 on April 26–27. Volume size distribution on April 27 exhibited a prominent coarse mode at 1–2 $\mu$m radius, and single-scattering albedo was observed to increase from 0.90 in the blue to 0.93 in the near infrared. Concurrent lidar observations tracked the evolution of the plume vertical structure, which consisted of up to three well-defined layers distributed throughout the free troposphere.

## 1. Introduction

During the closing days of April 1998 a particularly noteworthy instance of incursion by Asian-sourced dust was observed along the extent of the U.S. western seaboard [*Husar et al*., this issue]. Transport of Asian dust into the Pacific basin is a common occurrence during the northern spring, when strong cold fronts and convection over the Asian interior deserts loft crustal material into the midtroposphere [*Shaw*, 1980; *Duce et al*., 1980]. This material is frequently transported beyond the Hawaiian archipelago, on occasion penetrating the continental United States as far as the plains states. The frequency, duration, and strength of these dust events have been observed to be declining in recent decades due primarily to a Chinese government reforestation program aimed at reducing the detrimental economic and social impact of the dust storms [*Parungo et al*., 1994]. Notwithstanding this fact and despite observational support for a long-term downward trend in overall atmospheric aerosol loading [*Menzies and Tratt*, 1995], there still occur extreme Asian dust events. In the case of the April 1998 event the abnormal strength of the initiating storm generated an atypically dense cloud of material which resulted in dramatically reduced visibility along the length of the western seaboard (a collection of subjective reports describing such observations can be found at URL capita.wustl.edu/Asia-FarEast/). It has been recognized for some time that the very size of the dust storms implies a significant, nonnegligible radiative forcing impact which merits more intensive study [e.g., *Charlson et al*., 1982; *Golitsyn and Gillette*, 1993].

In addition to the climatic importance of these events, there may also be significant public health issues associated with cotransport of pathogens admixed with the refractory material comprising the bulk of the dust plumes. The central Asian desert regoliths are known to harbor infectious microorganisms as a result of their endemic presence among the local faunal population [*Burdelov and Pole*, 1984], and there is some anecdotal evidence from the Hawaiian islands linking epidemics characterized by influenza-like symptoms to the passage of Asian-sourced dust.

The purpose of this paper is to present observations of the April 1998 event from several platforms located in southern California. These data are from lidar, Sun photometer, and radiosondes. Additionally, transport simulations are presented to understand how the dust arrived in southern California. Analyzed together, the data reveal the details of a large-scale, complex, multilayered dust system that otherwise would go unnoticed by the individual platforms. Finally, this study demonstrates the benefits that can result from improved coordination of distributed observation networks.



Paper number 2000JD900758.
0148-0227/01/2000JD900758$09.00

## 2. Data Sources

### 2.1. Jet Propulsion Laboratory Coherent Backscatter Lidar

The Jet Propulsion Laboratory (JPL) coherent $CO_2$ backscatter lidar (operating wavelength 10.6 $\mu$m) has been in almost continuous operation since 1984 and has now accumulated a significant time series database tracking the long-term and seasonal variability of backscatter from the atmospheric column above the Pasadena, California, locale [*Tratt and Menzies*, 1994]. The lidar station site at 34° 12′ N, 118° 10′ W, 390 m mean sea level (msl) renders it suitable for the study of air masses advected from the Pacific basin before they are significantly modified by continental influences, since the prevailing

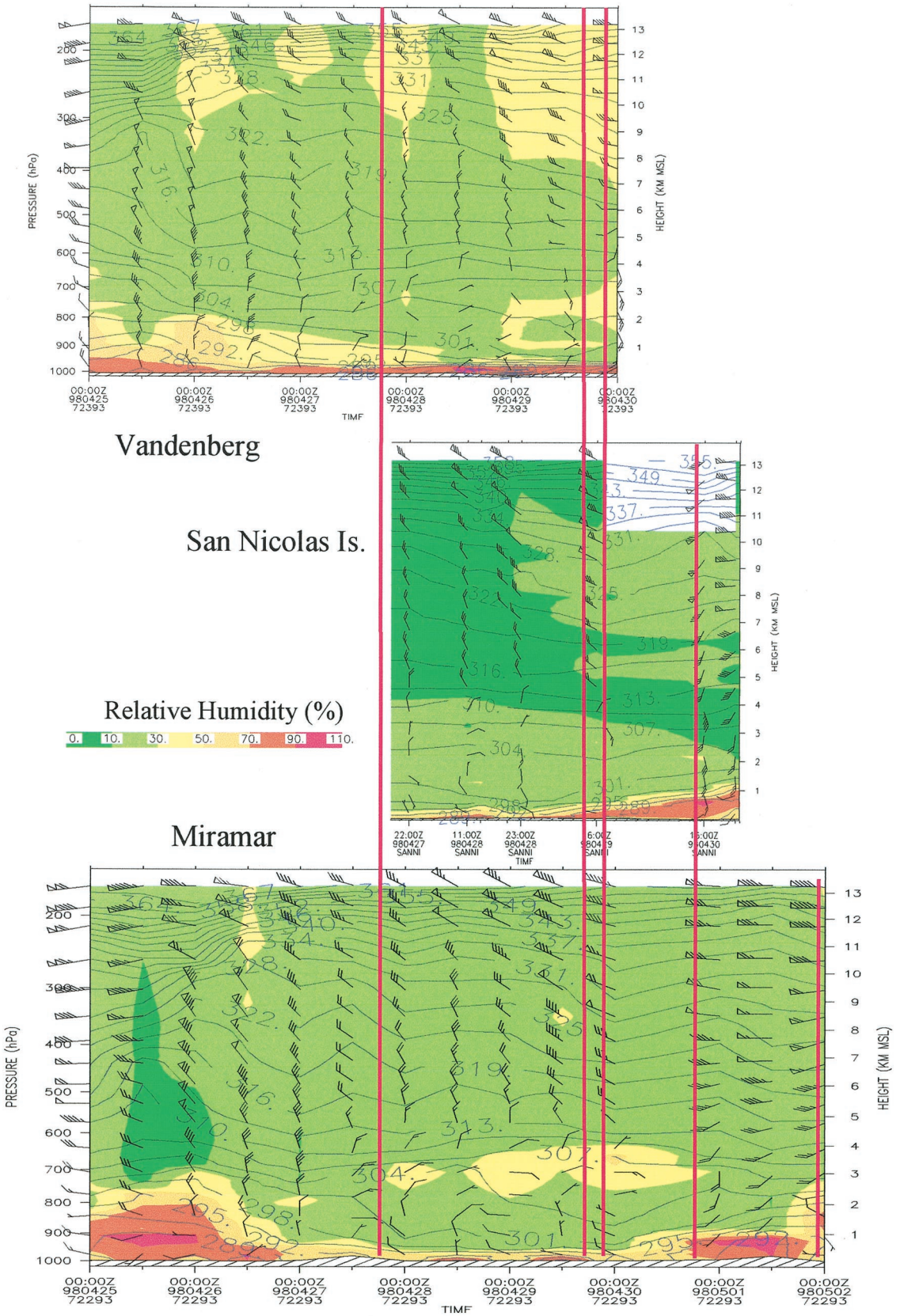


**Plate 1.** Time-height radiosonde records during the Asian dust episode. Relative humidity is color-coded from zero to 110%, labeled contours are potential temperature in Kelvin, and wind barbs are calibrated at 5 m/s per full barb. Time increases left to right and the vertical magenta lines denote the acquisition times of the lidar profiles depicted in Figure 2.

flow into the region is generally westerly [*Menzies et al*., 1989]. However, this statement only holds true above the planetary boundary layer, since contamination from the Greater Los Angeles urban/industrial plume is a major component of the total aerosol loading within this zone.

The JPL lidar was established with a charter to provide climatological-scale measurements of vertically resolved absolute backscatter (resolution ~200 m) throughout the troposphere and lower stratosphere. The inversion algorithm and radiometric calibration procedure that were developed in order to accomplish this requirement are described by *Kavaya and Menzies* [1985] and *Ancellet et al*. [1988], while the system itself is described by *Menzies et al*. [1984].

### 2.2. San Nicolas Island Sun Photometer

The NASA AERONET (Aerosol Robotic Network) is a globally distributed series of autonomously operated Sun photometer stations for the purpose of systematic aerosol data collection to aid in climatology research [*Holben et al*., 1998]. As part of this network, an autonomous Sun-sky scanning spectral radiometer is sited on San Nicolas Island off the California coast at geographical coordinates 33°15′ N, 119°29′ W, 133 m msl. The radiometer, developed by CIMEL Electronique (Paris, France), measures Sun and sky radiance, including solar aureole, in spectral bands centered at 1020, 870, 670, 500, 440, 380, and 340 nm and in the water vapor band at 940 nm (not used in the present study). The spectral bands are 10 nm wide and the instrument field of view is 1.2°. Pointing accuracy is 0.05°. The instrument is powered by solar panels and acquires data automatically. It activates at preprogrammed times and enters standby mode after each measurement sequence (Sun viewing, sky viewing in the almucantar and principal plane). Once every hour, the data are transmitted via the Geostationary Data Collection System to the NASA Wallops Flight Facility and processed in quasi-real-time at the NASA Goddard Space Flight Center. Data products are estimates of aerosol optical thickness and, using the *Dubovik and King* [2000] inversion technique, volume size distribution between 0.05 and 15 $\mu$m (particle radius), index of refraction (real and imaginary parts), single-scattering albedo, and phase function. The size distributions are vertical integrals through the atmosphere [see *Nakajima et al*., 1983]. The retrievals, however, may not be accurate when aerosol loadings are small (i.e., optical thickness at 500 nm below 0.1), as the sensitivity analysis of *Dubovik et al*. [2000] indicates.

### 2.3. NRL Aerosol Analysis and Prediction System

The Naval Research Laboratory (NRL) in Monterey, California, maintains a near real-time operational system for simulating the global distribution of tropospheric sulfate, dust, and smoke aerosols. Called the NRL Aerosol Analysis and Prediction System (NAAPS), this global model is a modified form of the hemispheric model of sulfate aerosols developed by *Christensen* [1997]. The NRL version uses global meteorological analyses and forecasts from the Navy Operational Global Atmospheric Prediction System (NOGAPS) [*Hogan and Rosmond*, 1991; *Hogan and Brody*, 1993] on a 1° × 1° grid, at 6-hour intervals and 18 vertical levels reaching 10 km. Dust and smoke emissions, transformations, and sinks have been added to the model. NAAPS allows multiple size bins, though only a single size bin is used in this study since we are interested primarily in the smaller particles (diameter <4 $\mu$m) which are subject to long-range transport. The model is described by *Westphal* [2000].

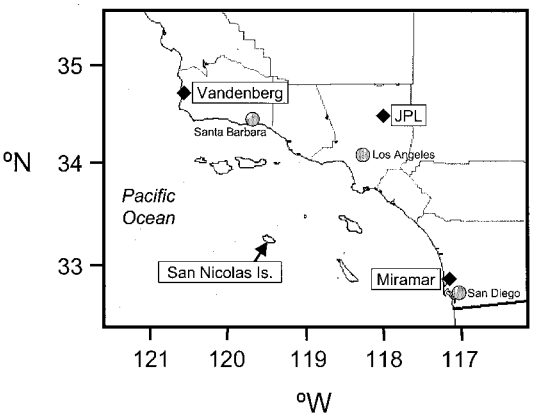


**Figure 1.** Geographic locations of observing stations contributing to the current study.

NAAPS has been operating since 1998 and is updated every 6 hours as each NOGAPS analysis becomes available. Every 12 hours a 5-day forecast is carried out. The global simulations of sulfate, dust, and smoke for various regions of the world are posted daily at URL www.nrlmry.navy.mil/aerosol along with daily satellite aerosol analyses for comparison purposes. In this paper, only the NAAPS analyses are used. These should provide the most accurate simulations since they are based on the NOGAPS analyses instead of the NOGAPS forecasts. However, the NAAPS analyses are actually aerosol forecasts since there is no data assimilation for aerosols.

## 3. Observations and Results

The synoptic conditions in southern California during the period of this study were characterized by a transition from westerly flow in a deep trough on April 25 to strong northerly flow in a steep ridge on April 26. The ridge persisted for several days, slowly weakening until a short wave passed through the region on April 30 and May 1, signaling the beginning of a rainy weather pattern. The significance of these synoptic features to the vertical structure of the atmosphere is illustrated in the radiosonde data from Vandenberg AFB (34°45′ N; 120°34′ W), San Nicolas Island, and Miramar NAS (32°52′ N; 117°9′ W). Figure 1 provides the geographical location of these stations (along with the JPL lidar site), while Plate 1 shows time-height sections of the data from these stations. Several features are generally present at all three stations. These include the two major transitions mentioned above and also three well-defined layers. At the first transition (arrival of the ridge) on April 25, westerly winds and a moderately stable atmosphere above 4 km (307 K isotherm) give way to northerly and NWN winds and a less stable atmosphere. This layer persists until the second transition (arrival of the short wave) on April 30 when it is replaced with westerly or SW winds and more stable conditions. The layer extends to the tropopause (334 or 331 K) which is at its highest altitude just after the ridge arrives, then slowly decreases in altitude until experiencing a slight elevation gain following the passage of the short wave.

The marine layer is deep at first, becoming quite shallow in the presence of the northerly flow, and then deepens again

after the passage of the short wave. A third layer appears between 0.5 and 3 km after the first transition and vanishes by May 1. It is well defined at Miramar but less so at the other two stations. It is weakly stable and topped by an inversion at the 307 K isotherm. The winds in this layer are weak and variable with northerly or easterly components. The northerly and easterly winds imply a continental, possibly polluted, boundary layer. The surface concentrations of dust at various West Coast sites indicated the presence of dust even at the surface. Hence this continental layer could also contain Asian dust, but the structure of the atmosphere indicates that it must have traveled along a much different pathway than that of the upper tropospheric layer.

The Vandenberg and San Nicolas time series are incomplete, but the similarities between the available data and those from Miramar allow us to infer that similar conditions existed at all stations from April 25 and May 1. Furthermore, the rawinsonde data from Edwards Air Force Base (130 km inland, not shown) also contained the same features, excluding the marine boundary layer.

To summarize, three significant layers existed during the period in question. These are the upper troposphere neutral layer, the lower-level continental layer, and the marine boundary layer. These layers are bounded by the tropopause and the surface and separated by two inversions. The location of the tropopause and the two inversions are noted on the lidar profiles shown in Figure 2. The acquisition times of the lidar profiles are shown with vertical bars in Plate 1.

The first JPL lidar observations of the event were acquired on April 27, 1998. The evolution of the dust layers was tracked in five lidar profiles taken throughout the week ending with the onset of stormy conditions on May 2. Table 1 shows the acquisition times of the five lidar profiles acquired during this period, while the retrieved backscatter profiles are shown in Figure 2. In this figure the dashed curves represent the computed noise-equivalent backscatter, corresponding to the point at which the signal level is indistinguishable from the system noise.

Concurrent visual observations during each lidar profile acquisition indicated that the atmosphere overhead appeared cloud free. Subjective observations of this kind can be misleading (especially under the very hazy conditions prevailing during this event), but the radiosonde data (Plate 1) also support the assumption of no cloud contamination. For the entire study period, the humidity aloft is less than 30% except for a few brief moister periods when the humidity still was less than 50%.

Strong scattering characterizes the upper level neutral layer. The top of the layer follows the behavior of the tropopause: slowly decreasing in altitude (profiles 1–3) then increasing (profile 4). The base is well defined by the inversion separating the two tropospheric layers. Considerable variability in the vertical structure and layering are present: a single deep layer being evident in profile 1, while multiple well-stratified layers appear in profiles 2–4. These layers have no readily apparent analogous features in the radiosonde data, but some of the features are consistent from profile to profile. For example, the same local maximum appears to be present at 6, 5.5, and 4.5 km msl in profiles 2, 3, and 4, respectively. These maxima appear near the base of the upper level neutral layer. The persistent presence of the scattering features in the lidar profiles at the 6–10 km msl altitude range (profiles 1-4) suggests continued presence of Asian dust in the Los Angeles area from April 27 to 30. The low-level continental layer is characterized by strong scattering in profiles 1–4. The large reduction in scattering in the free troposphere on May 1 coincides with the passage of the short wave and the disappearance of both the upper level near-neutral layer and the low-level continental layer (Plate 1).

The variation of aerosol optical thickness at 500 nm and Ångström coefficient between 380 and 1020 nm at San Nicolas Island over the April 18 to May 1, 1998, period are shown in Figure 3. The Ångström coefficients were determined by calculating, on a logarithm scale, the linear-square-fit slope of the spectral Sun photometer measurements (340–1020 nm) as a function of wavelength. Aerosol optical thickness increased markedly from 0.15 to 0.34 on April 25 and reached maximum values of 0.52 on April 26–27 (Figure 3a). During those days the Ångström coefficient was below 0.5 with minimum values of 0.2 on April 25 following the arrival of the dust (Figure 3b).

The dust event can be easily distinguished from the background conditions by examining the Ångström coefficient as a function of aerosol optical thickness (Figure 4). The background conditions are associated with an optical thickness of less than 0.2 and a variable Ångström coefficient (ranging from 0.3 to 1.6). The low Ångström coefficient values suggest some influence of continental aerosols or urban aerosols from the Los Angeles area. The dust event, on the other hand, is characterized by a higher optical thickness (above 0.2) and a fairly constant Ångström coefficient (0.2 to 0.4). The points in the top left-hand corner of the rectangle (Figure 4) depict the situation of May 1, 1998. Aerosol loading was higher than during the previous day, probably due to some residual dust patches, and mixing with more continental-type aerosols (higher accumulation mode) might have resulted in Ångström coefficients generally lower than those observed at the peak of the dust event. The Ångström coefficient is expected to be more negative for continental and pollution aerosols (for example, 1.4 is typically characteristic of a continental aerosol).

Figure 5 illustrates typical columnar volume size distribution retrievals at San Nicolas Island before (April 20), during (April 27), and toward the end of the event (April 30). This display clearly shows that the dust event is characterized by a prominent coarse mode at 1–2 $\mu$m radius, similar to measurements inferred in earlier studies of Asian dust arriving in Hawaii [e.g., *Shaw*, 1980; *Braaten and Cahill*, 1986]. This value is much lower than the dominant sizes of above 10 $\mu$m observed at the source in the Gobi desert [*Husar et al*., this issue], indicating that the larger particles were lost during transport over the Pacific Ocean. The April 27 size distribution also exhibits a strong accumulation mode, which may have contributed to lower the Ångström coefficient. Before and after the dust event the distributions do not exhibit a large peak at 1–2 $\mu$m radius, but it is difficult to interpret further the observed modes, which may result from various aerosol types and mixtures. The peak at about 7 $\mu$m appearing in the April 20 distribution may possibly be due to undetected thin, homogeneous clouds.

The single-scattering albedo spectra for the three cases of Figure 5 are displayed in Figure 6. Before the dust event (April 20), single-scattering albedo decreased with wavelength, suggesting some residual continental (or possibly urban) influence. This is consistent with the size distribution and extinction data discussed above. During the dust event, single-scattering albedo was lower in the blue, with values of 0.90 at 440 nm and 0.93 at 1020 nm. Coupling between molecular scattering and this aerosol absorption, by darkening the aerosol reflectance in

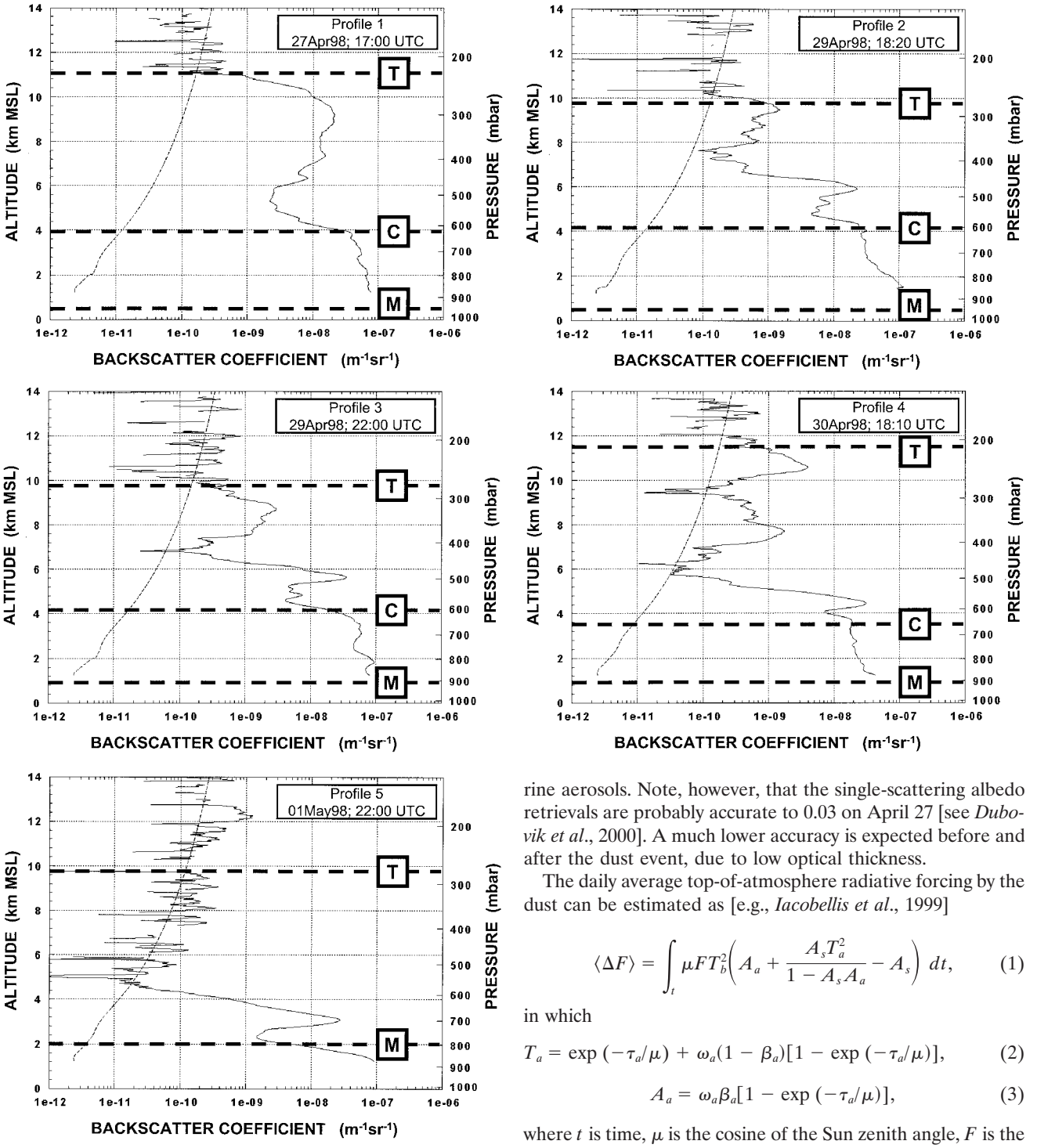


**Figure 2.** Absolute backscatter profiles of the Asian dust event acquired by the JPL lidar. The individual panel legends correspond to Table 1. The thin broken curves denote the altitude-dependent effective system sensitivity. The thick broken horizontal lines denote the positions of salient temperature inversions discussed in the text: T, tropopause; C, continental inversion; M, marine boundary layer inversion.

the blue, may be a factor explaining the yellow aspect of the dust reported elsewhere [*Husar et al.*, this issue]. Following the dust event, the single-scattering albedo appeared somewhat invariant with wavelength, with a value of 0.99 typical of marine aerosols. Note, however, that the single-scattering albedo retrievals are probably accurate to 0.03 on April 27 [see *Dubovik et al.*, 2000]. A much lower accuracy is expected before and after the dust event, due to low optical thickness.

The daily average top-of-atmosphere radiative forcing by the dust can be estimated as [e.g., *Iacobellis et al.*, 1999]

$$\langle \Delta F \rangle = \int_t \mu F T_b^2 \left( A_a + \frac{A_s T_a^2}{1 - A_s A_a} - A_s \right) dt, \qquad (1)$$

in which

$$T_a = \exp(-\tau_a/\mu) + \omega_a(1 - \beta_a)[1 - \exp(-\tau_a/\mu)], \qquad (2)$$

$$A_a = \omega_a \beta_a [1 - \exp(-\tau_a/\mu)], \qquad (3)$$

where $t$ is time, $\mu$ is the cosine of the Sun zenith angle, $F$ is the extraterrestrial solar irradiance, $A_a$ is the reflectivity of the dust layers and $T_a$ their transmissivity, $\omega_a$ is the dust single-scattering albedo, $\beta_a$ is the upward fraction of the flux scattered by the dust (a function of $\mu$), $\tau_a$ is the dust optical thickness, $T_b$ is the transmissivity of the atmosphere without dust (background conditions), and $A_s$ is the surface albedo. In (1) the time integral is over 1 day.

Using for $\tau_a$, $\omega_a$, and $\beta_a$ the CIMEL radiometer values weighted by the extraterrestrial spectral solar irradiance, setting $A_s = 0.06$, and assuming that $T_b$ is due only to molecular scattering and absorption (i.e., neglecting the aerosol background), we obtain $\langle \Delta F \rangle = 28.2$ W m$^{-2}$ on April 27. Thus the dust, which persisted for several days and was extended spa-

**Table 1.** Summary of Lidar Data Used in the Current Study

| Lidar Profile | Date | Lidar Accumulation Interval, UTC |
|---|---|---|
| 1 | 27Apr98 (day117) | 1630–1730 |
| 2 | 29Apr98 (day119) | 1750–1850 |
| 3 | 29Apr98 (day119) | 2130–2230 |
| 4 | 30Apr98 (day120) | 1740–1840 |
| 5 | 01May98 (day121) | 2130–2230 |

Read 27Apr98 as April 27, 1998.

tially, may have exerted a significant cooling influence off the California coast. Over land, because the surface albedo is much higher than 0.06, aerosol absorption can reduce the reflected solar flux exiting the atmosphere (warming influence), but in our case, this would have required a single-scattering albedo much smaller than 0.9–0.93 (Figure 6), of the order of 0.8 or less.

NAAPS is used to assist in interpreting the observations, after demonstrating that it accurately simulates the dust event.

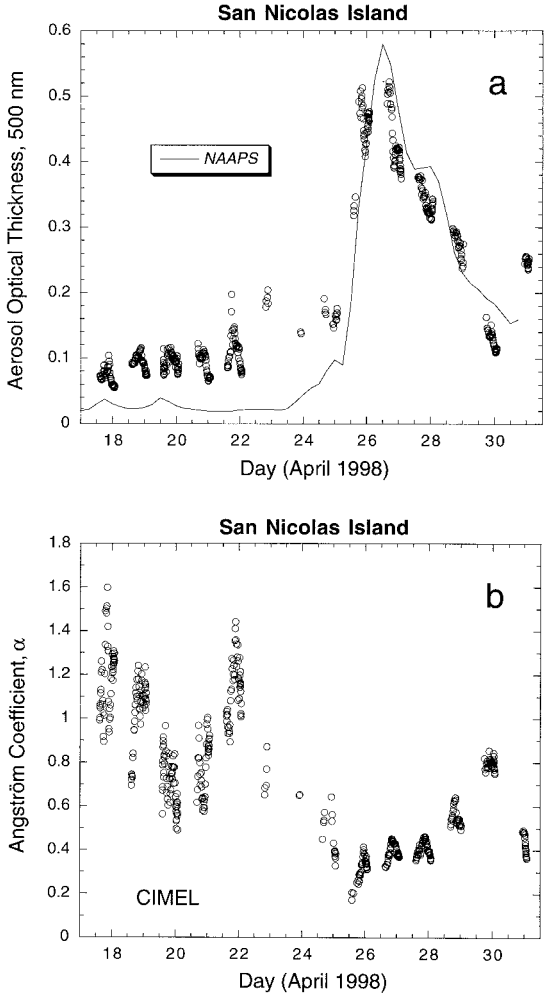


**Figure 3.** Time series of (a) aerosol optical thickness at 500 nm and (b) Ångström coefficient between 380 and 1020 nm at San Nicolas Island during April 18 to May 1, 1998. Figure 3a also shows simulated optical depth (× 0.25) of dust and sulfate from NAAPS.

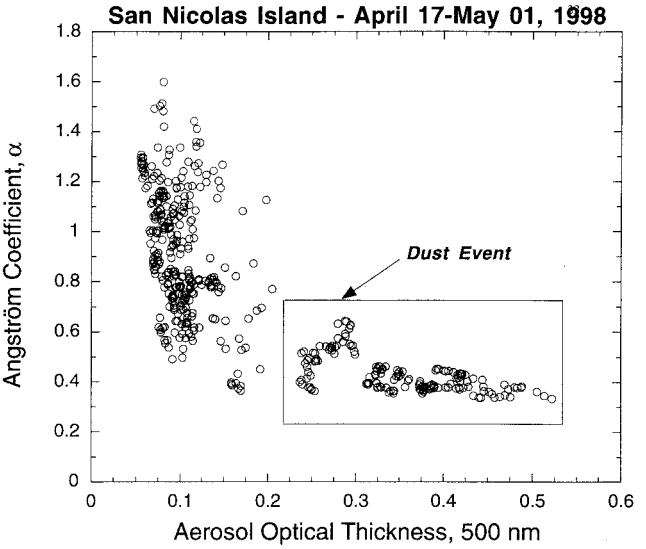


**Figure 4.** Ångström coefficient between 380 and 1020 nm versus aerosol optical thickness at 500 nm at San Nicolas Island during April 18 to May 1, 1998. Points characterized by aerosol optical thickness above 0.22 and Ångström coefficient below 0.5 delineate the dust event.

In Plate 2 we compare the Total Ozone Mapping Spectrometer (TOMS) absorbing aerosol index (AI) operational product [*Herman et al*., 1997] with the NAAPS dust optical depths. The TOMS AI shows the progression of the dust across the Pacific between 30° N and 50° N, with occasional incursions over Alaska. The dust cloud arrives at the West Coast on April 25 and lingers until April 30. The void trailing the main body of the dust plume which is evident in the TOMS retrievals of April 24 and 25 may be real or could be due to suppression of the AI values in the presence of water clouds. The NAAPS aerosol optical depths (AOD) show good agreement with the AI values in terms of distribution and timing, including the

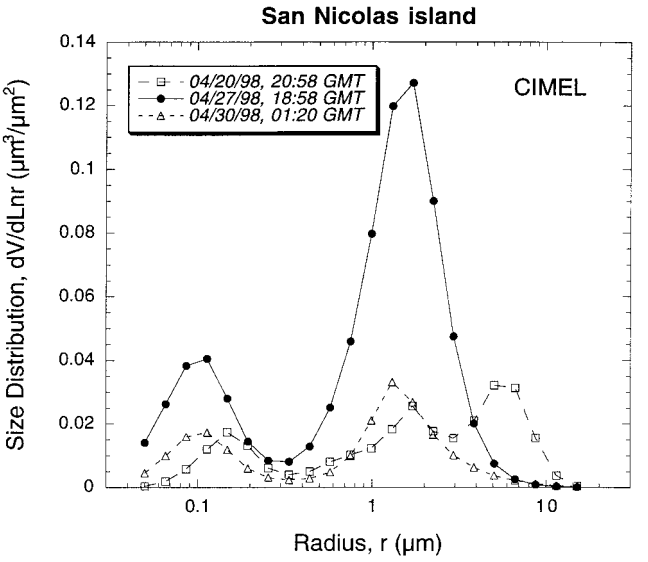


**Figure 5.** Typical volume size distributions retrieved from AERONET AOD measurements at San Nicolas Island before the dust event (April 20), during the dust event (April 27), and after the dust event (April 30).

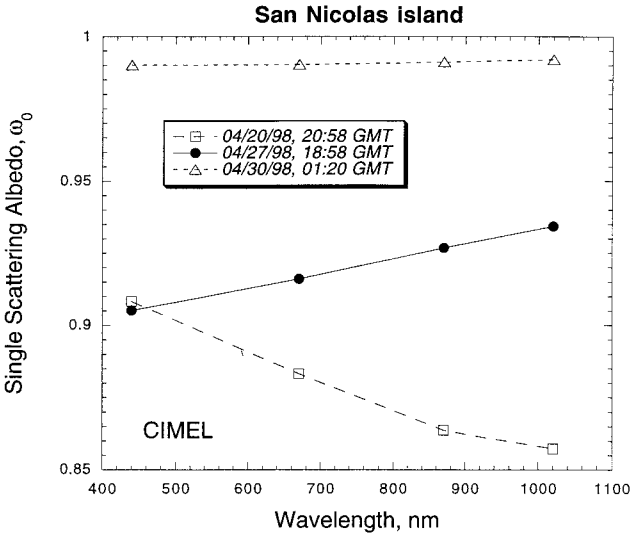


**Figure 6.** Single-scattering albedo versus wavelength for the three cases of Figure 5.

dust over Alaska, the peak values along the coast on April 25 and 26, and the slow dissipation through April 30.

The skill of the model is illustrated by comparing the AOD with the AERONET data in Figure 3a. NAAPS captures the sudden onset and the gradual decay of the dust event. However, the AOD values in the figure have been scaled by 0.25, that is, NAAPS overestimates the AOD by a factor of 4. Since the timing and shape of the event are so well modeled, the overestimate is most likely due to errors in the dust source term or removal mechanisms, as opposed to transport errors. NAAPS does not accurately simulate the magnitude of the background aerosol prior to April 25. Without scaling, the sulfate AOD values during this period would have been between 0.025 and 0.04. The addition of locally derived nonsulfate aerosols, including salt, could easily account for the difference between NAAPS and the Sun photometer data during this period. Regardless, NAAPS does capture the distribution and timing of the dust event.

The most relevant NAAPS product is the evolution of the vertical distribution of aerosol for the grid point nearest the JPL lidar in Pasadena. This distribution is shown in Plate 3 along with the NOGAPS fields of potential temperature and winds and the approximate location of the scattering layers shown in Figure 2. Comparison with the radiosonde data in Plate 1 shows that NOGAPS captures the two transitions on April 25 and 30 and the upper troposphere neutral layer and low-level continental layer. The marine boundary layer is not evident at this inland location. NAAPS shows the sudden onset of high dust concentrations coinciding with the arrival of the upper level neutral layer behind the steep ridge on April 25. (Recall that these concentrations are possibly 4 times too high.) This represents the arrival of the north-south tongue of dust seen in Plate 2 on April 24 along 140°W. The dust fills the upper level neutral layer from the tropopause to the inversion separating the upper level neutral layer and the low-level continental layer. The highest concentrations and deepest dust layer occur at 1200 UTC on April 26, in agreement with the AERONET data for San Nicolas Island (Figure 3a). From April 27 to 30 the concentrations slowly decrease, and the top sinks over the next day. The AERONET optical depths likewise slowly decrease. NAAPS shows the low-level continental layer to be apparently dust free. The high scattering seen in this layer by the JPL lidar is apparently due to some other aerosol, possibly from local pollution sources. The dust event terminates sometime after April 30.

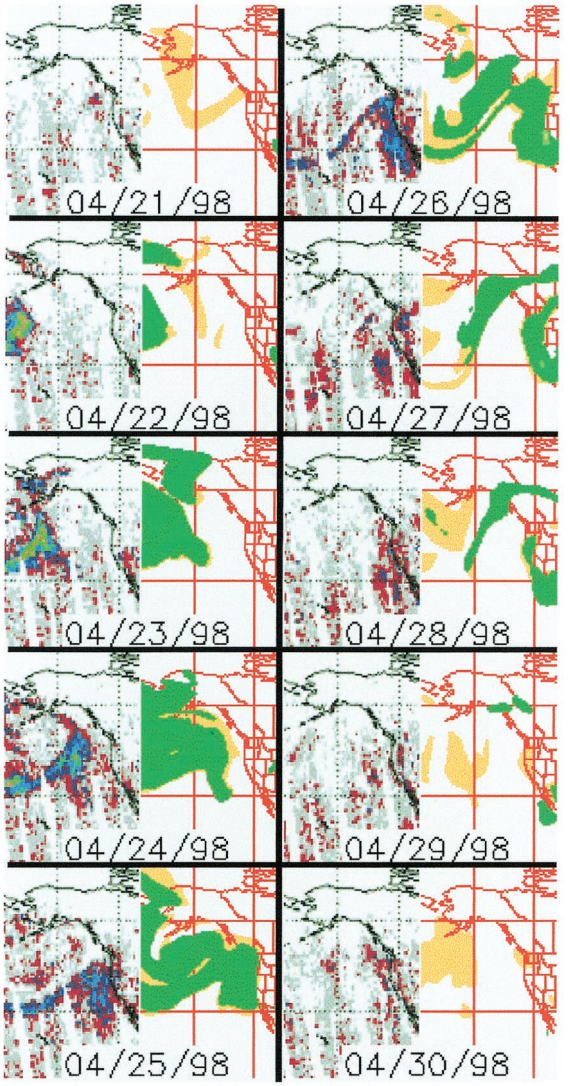


**Plate 2.** Transport synopsis of the Asian dust event, the magnitude of which can be gauged by reference to the superimposed continental outline of North America. The left-hand side of each panel shows the TOMS (absorbing) aerosol index, while the right-hand side indicates the modeled dust (green) and sulfate (orange) optical depths computed by NAAPS.

NAAPS simulates many of the characteristics of the dust event but not the detailed vertical distribution evident from the lidar data (Plate 3). This is likely due to poor vertical resolution. The wind barbs in Plate 3 indicate the approximate locations of the model layers. The coarse vertical resolution does not, however, explain the absence of the layer of dust located near the top of the troposphere on April 29 and 30 (lidar profiles 2–4 in Figure 2). It is clearly possible that this feature relates to some more localized phenomenon, but in the absence of additional data to support such a conjecture, there is currently no verifiable means to account for this discrepancy. Back trajectories from this altitude show origins over China 9–10 days earlier [*Perry et al.*, 1999], coinciding with the pas-

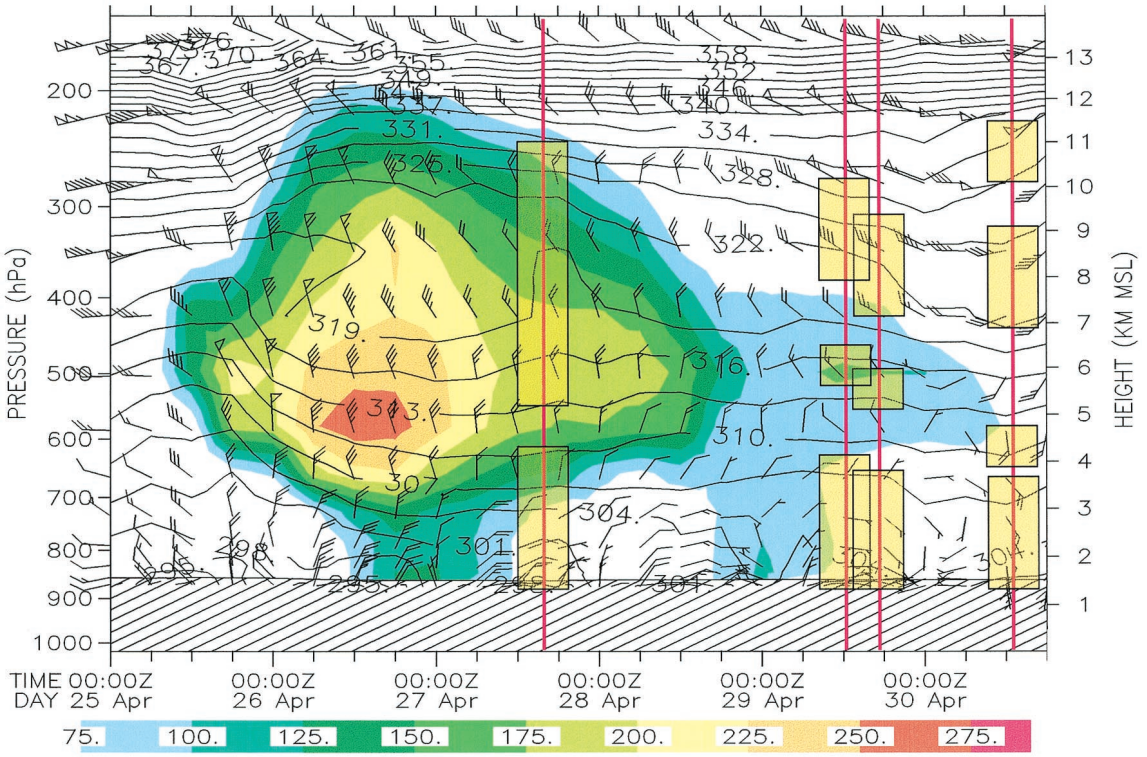


**Plate 3.** Time-height display of NAAPS and NOGAPS data for the grid point nearest Pasadena (34.5° N; 118° W) during the Asian dust episode, April 25–30, 1998. Dust concentration is color-coded from 100 to 300 $\mu$g m$^{-3}$, labeled contours are potential temperature in Kelvin, and wind barbs are calibrated at 5 m/s per full barb. Time increases left to right, and the vertical magenta lines denote the acquisition times of the lidar profiles depicted in Figure 2. The boxes associated with each lidar profile marker delineate the altitudes where the most prominent lidar-detected layers reside. Compare with the radiosonde data shown in Plate 1.

sage through that region on April 19 of a rapidly moving shallow trough which, through analysis of surface observations and satellite imagery, has been identified as the chief progenitor of the eastward transported dust [*Westphal et al.*, 1998].

The very high aerosol concentrations modeled for April 26 and detected by the AERONET Sun photometer occurred before notification of the event had been received at JPL, with the result that supporting lidar data for the peak period are not available. A more complete analysis of this event would have been possible if the alert had been issued earlier. It is anticipated that similar events in the future will be amenable to more detailed observation as a result of the electronic notification medium which came about as a result of the April 1998 event [*Husar et al.*, this issue].

## 4. Conclusion

We have described the results of a multisensor investigation of the severe Asian dust event that reached the west coast of North America in April 1998. The combination of quasi-collocated complementary data sets and transport modeling permits covalidation of retrieval and model fidelity and enhanced accuracy of the associated radiative forcing contribution.

The progress of the April 1998 dust cloud eastward across the Pacific Ocean was initially detected in satellite imagery and the broader atmospheric research community was subsequently notified via electronic communications. Use of the Internet medium in this way was effective in facilitating a rapid-response correlative measurement exercise by numerous atmospheric observation stations throughout the western United States, and its success has resulted in the establishment of an ad hoc communications environment, data exchange medium, and mechanism for providing early warning alert of other significant atmospheric phenomena in the future [*Husar et al.*, this issue].

The dust plume persisted for several days and comprised up to three distinct layers, at times occupying up to 6 km of the atmospheric column. The vertical structure is not resolvable in satellite retrievals of aerosol properties. However, range-resolved vertical backscatter profiles provided by lidar allowed for the detection and characterization of the layering present within the plume. In this respect the lidar data provided a unique resource for the verification of three-dimensional (3-D) transport simulations and were critical to a more comprehensive understanding of the event. Optical depth records acquired from San Nicolas Island reveal a dramatic increase in atmospheric opacity on April 25, 1998, which transport simulations suggest corresponded to the first arrival of the dust plume in the locale. Aerosol size distributions retrieved from the optical depth measurements exhibited a prominent coarse mode at 1–2 $\mu$m radius during the dust event.

While the April 1998 episode was remarkably intense, subsequent continuous observation of satellite imagery and continuous NAAPS simulations reveal numerous Asian dust events each spring with dust from several of these reaching North America, the occurrence of which was suggested in

earlier reports [*Menzies et al*., 1989; *Tratt and Menzies*, 2000]. Regardless of these prior indicators, no event of comparable magnitude was recorded during the 15-year history of the lidar archive. The exceptional prominence of the 1998 episode has resulted in greater awareness of the potential for significant Asian dust incursions into the southern California locale and a more integrated, less ad hoc, approach to their observation and study.

Since both the dust and the pollution have surface sources, it is understandable that pollutants are present with the dust transported to North America [e.g., *Jaffe et al*., 1999; *Berntsen et al*., 1999]. One of the most surprising aspects of these events is that surface-based aerosols can be elevated to altitudes of ~10 km and transported thousands of kilometers without appreciable scavenging by precipitation. Thus the detection and characterization of these events and the dynamics behind the transport take on greater importance in light of the expected modernization and industrial development of the Far East.

**Acknowledgments.** Portions of this work were carried out by the Jet Propulsion Laboratory, California Institute of Technology, under contract with the National Aeronautics and Space Administration (NASA), with the support of Ramesh Kakar, Atmospheric Dynamics and Remote Sensing Program, NASA Office of Earth Science. NASA provided additional support under contracts NAS-97135, NAG5-6202, and NAS5-97135. The support of the Office of Naval Research and the Naval Research Laboratory through programs PE-0602435N and PE-06-1153 is gratefully acknowledged. Oleg Dubovik, Alexander Smirnov, and Ilya Slutsker of the NASA Goddard Space Flight Center AERONET team are gratefully acknowledged for provision and validation of columnar aerosol size distribution retrievals. Joyce Borgen of the Naval Air Warfare Station, Point Mugu, California, provided radiosonde data for San Nicolas Island. TOMS data were supplied by Omar Torres, NASA Goddard Space Flight Center.

## References

Ancellet, G. M., R. T. Menzies, and D. M. Tratt, Atmospheric backscatter vertical profiles at 9.2 and 10.6 μm: A comparative study, *Appl. Opt*., *27*(23), 4907–4912, 1988.

Berntsen, T. K., S. Karlsdóttir, and D. A. Jaffe, Influence of Asian emissions on the composition of air reaching the northwestern United States, *Geophys. Res. Lett*., *26*(14), 2171–2174, 1999.

Braaten, D. A., and T. A. Cahill, Size and composition of Asian dust transported to Hawaii, *Atmos. Environ*., *20*(6), 1105–1109, 1986.

Burdelov, A. S., and S. B. Pole, Influence of human activity on the natural plague focus in the central Asian desert, *Sov. J. Ecol*., *15*(3), 142–145, 1984.

Charlson, R. J., T. Silver, A. D. Clarke, and B. A. Bodhaine, Comments on "Transport of Asian desert aerosol to the Hawaiian Islands," *J. Appl. Meteorol*., *21*(11), 1775–1776, 1982.

Christensen, J. H., The Danish Eulerian hemispheric model—A three-dimensional air pollution model used for the Arctic, *Atmos. Environ*., *31*(24), 4169–4191, 1997.

Dubovik, O., and M. D. King, A flexible inversion algorithm for retrieval of aerosol optical properties from Sun and sky radiance measurements, *J. Geophys. Res*., *105*, 20,673–20,696, 2000.

Dubovik, O., A. Smirnov, B. N. Holben, M. D. King, Y. F. Kaufman, T. F. Eck, and I. Slutsker, Accuracy assessments of aerosol optical properties retrieved from Aerosol Robotic Network (AERONET) Sun and sky radiance measurements, *J. Geophys. Res*., *105*, 9791–9806, 2000.

Duce, R. A., C. K. Unni, B. J. Ray, J. M. Prospero, and J. T. Merrill, Long-range atmospheric transport of soil dust from Asia to the tropical North Pacific: Temporal variability, *Science*, *209*, 1522–1524, 1980.

Golitsyn, G., and D. A. Gillette, Introduction: A joint Soviet-American experiment for the study of Asian desert dust and its impact on local meteorological conditions and climate, *Atmos. Environ*., *27A*(16), 2467–2470, 1993.

Herman, J. R., P. K. Bhartia, O. Torres, N. C. Hsu, C. J. Seftor, and E. Celarier: Global distribution of UV-absorbing aerosols from Nimbus 7/TOMS data, *J. Geophys. Res*., *102*, 16,911–16,922, 1997.

Hogan, T. F., and L. R. Brody, Sensitivity studies of the Navy global forecast model parameterizations and evaluation of improvements to NOGAPS, *Mon. Weather Rev*., *121*(8), 2373–2395, 1993.

Hogan, T. F., and T. E. Rosmond, The description of the Navy operational global atmospheric prediction system's spectral forecast model, *Mon. Weather Rev*., *119*(8), 1786–1815, 1991.

Holben, B. N., et al., AERONET—A federated instrument network and data archive for aerosol characterization, *Remote Sens. Environ*., *66*(1), 1–16, 1998.

Husar, R. B., et al., Asian dust events of April 1998, *J. Geophys. Res*., this issue.

Iacobellis, S. F., R. Frouin, and R. C. J. Somerville, Direct climate forcing by biomass burning aerosols: Impact of correlations between controlling variables, *J. Geophys. Res*., *104*, 12,031–12,045, 1999.

Jaffe, D., et al., Transport of Asian air pollution to North America, *Geophys. Res. Lett*., *26*(6), 711–714, 1999.

Kavaya, M. J., and R. T. Menzies, Lidar aerosol backscatter measurements: Systematic, modeling, and calibration error considerations, *Appl. Opt*., *24*(21), 3444–3453, 1985.

Menzies, R. T., and D. M. Tratt, Evidence of seasonally dependent stratosphere-troposphere exchange and purging of lower stratospheric aerosol from a multiyear lidar data set, *J. Geophys. Res*., *100*, 3139–3148, 1995.

Menzies, R. T., M. J. Kavaya, P. H. Flamant, and D. A. Haner, Atmospheric aerosol backscatter measurements using a tunable coherent $CO_2$ lidar, *Appl. Opt*., *23*(15), 2510–2517, 1984.

Menzies, R. T., G. M. Ancellet, D. M. Tratt, M. G. Wurtele, J. C. Wright, and W. Pi, Altitude and seasonal characteristics of aerosol backscatter at thermal infrared wavelengths using lidar observations from coastal California, *J. Geophys. Res*., *94*, 9897–9908, 1989.

Nakajima, T., M. Tanaka, and T. Yamauchi, Retrieval of the optical properties of aerosols from aureole and extinction data, *Appl. Opt*., *22*(19), 2951–2959, 1983.

Parungo, F., Z. Li, X. Li, D. Yang, and J. Harris, Gobi dust storms and The Great Green Wall, *Geophys. Res. Lett*., *21*(11), 999–1002, 1994.

Perry, K. D., T. A. Cahill, R. C. Schnell, and J. M. Harris, Long-range transport of anthropogenic aerosols to the National Oceanic and Atmospheric Administration baseline station at Mauna Loa Observatory, Hawaii, *J. Geophys. Res*., *104*, 18,521–18,533, 1999.

Shaw, G. E., Transport of Asian desert aerosol to the Hawaiian Islands, *J. Appl. Meteorol*., *19*(11), 1254–1259, 1980.

Tratt, D. M., and R. T. Menzies, Recent climatological trends in atmospheric aerosol backscatter derived from the Jet Propulsion Laboratory multiyear backscatter profile database, *Appl. Opt*., *33*(3), 424–430, 1994.

Tratt, D. M., and R. T. Menzies, The JPL 15-year lidar backscatter archive: A retrospective in *Proceedings of the Symposium on Lidar Atmospheric Monitoring*, pp. 15–18, Am. Meteorol. Soc., Boston, Mass., 2000.

Westphal, D. L., Real-time applications of a global multi-component aerosol model, *J. Geophys. Res*., in press, 2000.

Westphal, D. L., T. F. Hogan, and M. Liu, Dynamical forcing of the Chinese dust storms of April 1998, *Eos Trans. AGU*, *79*(45), Fall Meet. Suppl., F100, 1998.

R. J. Frouin, Scripps Institution of Oceanography, University of California, San Diego, 9500 Gilman Drive, La Jolla, CA 92093-0221.

D. M. Tratt, Jet Propulsion Laboratory, California Institute of Technology, MS 168-214, 4800 Oak Grove Drive, Pasadena, CA 91109-8099. (dtratt@jpl.nasa.gov)

D. L. Westphal, Marine Meteorology Division, Naval Research Laboratory, 7 Grace Hopper Avenue, Monterey, CA 93943-5502.

(Received January 24, 2000; revised September 19, 2000; accepted November 7, 2000.)